0026-895X/99/061207-12

MOLECULAR PHARMACOLOGY, **56:**1207–1218 (1999).

Putative Partial Agonist 1-Aminocyclopropanecarboxylic Acid Acts Concurrently as a Glycine-Site Agonist and a Glutamate-Site Antagonist at *N*-Methyl-D-aspartate Receptors

RINAT NAHUM-LEVY, LINDA H. FOSSOM,[1] PHIL SKOLNICK,[2] and MORRIS BENVENISTE

Department of Physiology and Pharmacology, Sackler School of Medicine, Tel Aviv University, Ramat Aviv, Israel (R.N.-L., M.B.); and Laboratory of Neuroscience, National Institute of Diabetes and Diseases of the Kidney, National Institutes of Health, Bethesda, Maryland (L.H.F., P.S.)

Received July 6, 1999; accepted August 28, 1999

This paper is available online at http://www.molpharm.org

ABSTRACT

1-Aminocyclopropanecarboxylic acid (ACPC) has been shown to protect against neuronal cell death after ischemic insult in vivo. Such results can be correlated with in vitro assays in which ACPC protected neurons against glutamate-induced neurotoxicity by reducing the activity of *N*-methyl-D-aspartate (NMDA) channel activation. Electrophysiological studies have determined that ACPC inhibits NMDA receptor activity by acting as a glycine-binding site partial agonist. In this study, rapid drug perfusion combined with whole-cell voltage-clamp was used to elicit and measure the effects of ACPC on NMDA receptor-mediated responses from cultured hippocampal neurons and cerebellar granule cells. The ACPC steady-state dose-response curve had both stimulatory and inhibitory phases. Half-maximal activation by ACPC as a glycine-site agonist was 0.7 to 0.9 μM. Half-maximal inhibition by ACPC was dependent on NMDA concentration. Peak responses to a $>$100 μM ACPC pulse in the presence of 1 μM glutamate were similar to those of glycine but decayed to a steady-state amplitude below that of glycine. The removal of ACPC initially caused an increase in inward current followed by a subsequent decrease to baseline levels. This suggests that relief of low-affinity antagonism occurs before high-affinity agonist dissociation. Simulations of ACPC action by a two glutamate-binding site/two glycine-binding site model for NMDA channel activation in conjunction with the concurrent role of ACPC as a glycine-site full agonist and glutamate-site competitive antagonist were able to successfully approximate experimental results.

The extensive neuronal loss observed after ischemic insult has been attributed to a massive and sustained release of glutamate resulting from anoxic depolarization (reviewed in Szatkowski and Attwell, 1994). Glutamate, in the presence of glycine, can cause activation of *N*-methyl-D-aspartate (NMDA) receptor cationic channels (Johnson and Ascher, 1987; Kleckner and Dingledine, 1988). Because these channels have a high permeability for calcium ions (Mayer and Westbrook, 1987; Schneggenburger et al., 1993), sustained activation of these channels can elevate levels of intracellular calcium to toxic levels (Garthwaite and Garthwaite, 1986; Hartley and Choi, 1989; Choi, 1992). NMDA antagonists reduce both glutamate-induced neurotoxicity in primary cell cultures (Hartley and Choi, 1989) and brain damage after ischemic insult in a variety of animal models (Meldrum, 1994). Based on this preclinical evidence, several NMDA antagonists are under evaluation for the treatment of ischemic insult (e.g., stroke and traumatic brain injury) in humans (Bigge and Boxer, 1994; Muir et al., 1994).

NMDA antagonists acting at distinct loci are effective in limiting ischemia-induced excitotoxic damage in animals (Bigge and Boxer, 1994). However, based on clinical observations with competitive NMDA receptor antagonists (e.g., 4-(3-phosphonoprop-2-enyl)piperazine-2-carboxylic acid) and use-dependent channel blockers (e.g., CNS 1102), both psychotomimetic-like side effects and memory impairment may limit their therapeutic potential (Sveinbjornsdottir et al., 1993; Muir et al., 1994; Rockstroh et al., 1996). These clinically undesirable actions of NMDA receptor antagonists may result from vastly reduced NMDA receptor/channel activation and ion flow (Rogawski, 1993; Parsons et al., 1995), preventing NMDA channel-mediated synaptic currents. The use of glycine partial agonists may minimize side effects by allowing a moderate level of NMDA receptor activation and normal synaptic transmission while attenuating excessive NMDA receptor activation leading to neurotoxicity (Maccecchini, 1995).

This work was supported by Grant 96-00245 from the United States-Israel Binational Science Foundation (Jerusalem, Israel) and by Grant 3765 from the Israeli Ministry of Health.

[1] Present address: Division of Neuropharmacological Drug Products, CDER/FDA, HFD-120, 5600 Fishers Lane, Rockville, MD 20857.

[2] Present address: Lilly Research Laboratories, Indianapolis, IN 46285.

ABBREVIATIONS: ACPC, 1-aminocyclopropanecarboxylic acid; NMDA, *N*-methyl-D-aspartate.

1-Aminocyclopropanecarboxylic acid (ACPC) has been shown to reduce neuronal damage in animal models of global (Fossom et al., 1995b) and spinal ischemia (Long and Skolnick, 1994). Furthermore, i.v. administration of ACPC produced no adverse side effects in humans (Cherkofsky, 1995) and no remarkable behavioral effects in rodents after doses as large as 2 g/kg (Skolnick et al., 1989).

In vitro electrophysiological and radioligand binding studies suggest that ACPC is a high-affinity, partial agonist acting at glycine agonist-binding sites on NMDA receptor ion channels with a 60 to 95% efficacy in comparison to saturating glycine (McBain et al., 1989; Watson and Lanthorn, 1990; Priestley and Kemp, 1994). Despite its relatively high efficacy as a glycine-site agonist, 1 mM ACPC elicits a ~50% reduction in glutamate neurotoxicity in granule neuron cultures (Boje et al., 1993; Fossom et al., 1995b). Interestingly, the efficacy of ACPC as a glycine-binding site agonist in both glutamate-induced neurotoxicity and NMDA-stimulated cGMP formation in cerebellar granule neuron cultures increased with increasing concentrations of glutamate (or NMDA) in these cultures (Fossom et al., 1995a,b). Interpretation of these assays, which measure the summed responses of a population of neurons in culture, may not be straightforward because the addition of glutamate agonists will cause neuronal depolarization and possible activation of voltage-gated ion channels in addition to activation of NMDA receptor ion channels. Nevertheless, these observations are consistent with the hypothesis that an inhibitory component of ACPC action may result from 1) an ACPC-dependent competitive inhibition of NMDA agonist binding or 2) an ACPC-mediated reduction in NMDA agonist binding through a non-agonist modulatory site.

By using rapid perfusion techniques in conjunction with whole-cell single-electrode voltage-clamp of cultured hippocampal neurons and cerebellar granule cells, we separated the actions of ACPC on NMDA ion channel activation into two kinetically distinct components: one stimulatory and one inhibitory.

Materials and Methods

ACPC used in these experiments was prepared via three different synthetic routes. ACPC purchased from Research Organics (Cleveland, OH) was synthesized from *N*-acetyl-DL-methioninate (Vaidyanathan and Wilson, 1989). Two lots of ACPC were donated by Symphony Pharmaceuticals (Malvern, PA). One lot was synthesized from cyclopropane-1,1-dicarboxylic acid dimethyl ester according to a method similar to that of Schubert (1990). A second lot was synthesized from α-bromo-γ-butyrolacetone according to a method similar to that described by Logusch (1986). All other chemicals were obtained from Sigma Chemical Co. (St. Louis, MO) unless otherwise indicated.

Neuronal Cultures. For low-density cultures of rat hippocampal neurons, two dissections were required: one to plate a layer of glial cells that sustain low-density neuronal growth, and a second dissection to plate neurons on top of the confluent layer of glial cells. For both dissections, seven Charles River postnatal day 1 newborn pups were decapitated, and hippocampi from both hemispheres were removed and digested with papain (100 U) for 20 min. After hippocampi were removed from the papain solution and triturated to a single-cell suspension, cells were plated at a density of 75,000 cells/ml onto 35-mm dishes. For the glial cell layer, the dishes were coated with calf skin collagen (50 μg/ml) and poly(L-lysine) (100 μg/ml), and cultures were grown in modified Eagle's medium containing 2 mM glutamine (Biological Industries, Kibbutz Beit HaEmek, Israel) and supplemented with 3.6 g/liter D-glucose, 10% fetal bovine serum, 100 U/ml penicillin, and 100 μg/ml streptomycin (Biological Industries). After ~10 days, a final concentration of 275 nM fluorodeoxyuridine and 680 nM uridine was added to the confluent glial cell layer to arrest cell division. Neurons were plated on top of this layer 2 weeks after the original dissection and grown in same culture medium described above except that the fetal bovine serum was replaced by 5% horse serum (Biological Industries).

For granule cell cultures, 6- to 8-day-old Sprague-Dawley rat pups were decapitated, and their cerebella were isolated as previously described (Gallo et al., 1982) with the exception that cytosine β-D-arabinofuranoside was not added. Cells were plated onto poly(D-lysine)-coated culture dishes and maintained in basal Eagle's medium containing 2 mM glutamine (GIBCO BRL), 25 mM KCl, 0.1 mg of gentamycin/ml, and 10% fetal bovine serum. All cultures were maintained at 36°C in humidified air containing 5% CO_2.

Electrophysiology and Rapid Perfusion System. Conventional whole-cell voltage-clamp experiments using an Axopatch 200A amplifier (Axon Instruments, Foster City, CA) were performed at room temperature at 1 to 2 weeks after neurons were plated. All experiments were conducted at a holding potential of −60 mV, unless indicated otherwise. The extracellular control solution consisted of 160 mM NaCl, 2.5 mM KCl, 0.2 mM $CaCl_2$, 10 mM glucose, 10 mM HEPES, 400 nM tetrodotoxin, 5 μM bicuculline methochloride, and 10 μg/ml phenol red and adjusted to pH 7.3 and 325 mOsm. The intracellular solution consisted of 125 mM $CsMeSO_3$, 15 mM CsCl, 0.5 mM $CaCl_2$, 3 mM $MgCl_2$, 5 mM Cs_4-1,2-bis(2-aminophenoxy)ethane-*N*,*N*,*N*′,*N*′-tetraacetic acid, and 2 mM Na_2ATP and adjusted to pH 7.2 and 305 mOsm.

For rapid application of agonist-containing solutions, a flowpipe consisting of an array of nine glass barrels (~400 μm o.d.) was positioned ~100 μm away from the neuronal soma, such that the flow from one of the barrels continuously bathed the entire neuron. At a given moment, a stepper motor positioned an adjacent barrel in front of the neuronal soma, and a different solution began to flow. Solution flow was controlled by solenoid valves that were driven by an Isolatch valve driver (Parker Hannifin, Fairfield, NJ). A Macintosh PPC 7600 computer with an ITC-16 analog-to-digital converter (Instrutech, Port Washington, NY) was used to synchronize stepper motor movement, valve opening, and data acquisition. The time constant for solution exchange was ~10 ms. Synapse, a Macintosh-based electrophysiological software package (Synergistic Systems, Silver Spring, MD), controlled data acquisition and was used for data analysis.

Concentration-Response Analysis. To determine a numerical description to characterize the biphasic nature of the ACPC concentration-response curve, the following multiple component logistic equation was used to determine half-maximal efficacy for activation ($E_{1/2}$) and inhibition ($I_{1/2}$):

$$100 \cdot \frac{I_{\mathrm{NMDA+ACPC}}}{I_{\mathrm{NMDA+Glycine}}} = \frac{\left(\left(\frac{[\mathrm{ACPC}]}{E_{1/2}}\right)^{n_1}\right)E_{\max}}{\left(1+\left(\frac{[\mathrm{ACPC}]}{E_{1/2}}\right)^{n_1}\right)\left(1+\left(\frac{[\mathrm{ACPC}]}{I_{1/2}}\right)^{n_2}\right)} \qquad (1)$$

where $I_{\mathrm{NMDA+ACPC}}$ and $I_{\mathrm{NMDA+Glycine}}$ are the steady-state amplitudes measured for currents activated by NMDA in the presence of the given concentration of ACPC or 10 μM glycine, respectively; $E_{\max}$ is the maximum efficacy of ACPC for the given concentration of NMDA; and n_1 and n_2 are the Hill coefficients for the stimulatory and inhibitory components of ACPC action, respectively. Equation 1 is used to fit the biphasic data shown in Fig. 2A without assuming a particular mechanism of action.

Equation 2 is a more standard dose-response equation with the exception that an offset has been added to account for a curve with a lower asymptote not equal to zero.

$$100 \cdot \frac{I_{\text{NMDA+ACPC}}}{I_{\text{NMDA+glycine}}} = \frac{E_{\max} - E_0}{1 + \left(\frac{E_{1/2}}{[\text{NMDA}]}\right)^{n_H}} + E_0 \quad (2)$$

In this case, $E_{1/2}$ represents the concentration of NMDA at which activation with a given concentration of ACPC yields a half-maximal efficacy, $E_{\max}$ is the maximal efficacy, n_H is the Hill coefficient, and E_0 is the degree of putative partial agonism that can be observed for ACPC at limiting NMDA concentrations. The number of variable parameters in eq. 2 was reduced to accommodate the limited number of data points in Fig. 2B. Thus, E_0 was determined from the relative efficacies of 7.5 and 15 μM ACPC in comparison with glycine (see Fig. 2B). This average was then used as a constant in the fit using eq. 2.

Equations 3 and 4 were used for standard concentration-response and concentration-inhibition analyses, respectively.

$$\text{Percent of control} = 100 \cdot \frac{I_{\max}}{1 + \left(\frac{\text{EC}_{50}}{[\text{drug}]}\right)^{n_H}} \quad (3)$$

$$\text{Percent of control} = 100 \cdot \frac{I_{\max}}{1 + \left(\frac{[\text{drug}]}{\text{IC}_{50}}\right)^{n_H}} \quad (4)$$

where $I_{\max}$ is the maximal response, EC_{50} is the concentration of the half-maximal stimulatory response, IC_{50} is the concentration of the half-maximal inhibitory response, and n_H is the Hill coefficient. All errors are standard deviations.

Simulations. Simulations were conducted on a Power Macintosh G3 computer using the program FastFlow, originally written by Dr. J. D. Clements (Benveniste et al., 1990) and extensively modified by M.B. This program simulates whole-cell currents under voltage-clamp by numerically calculating the probability of occupancy of each channel state assuming that transitions between states follow simple first order reaction kinetics.

Results

Initial efficacy estimates of ACPC were determined from measurements made in rat cerebellar granule cells at a holding potential of −60 mV using two concentrations of ACPC (10 μM and 1 mM) and NMDA (15 and 150 μM). Figure 1, A and B, illustrates responses in which a pulse of NMDA elicited currents in the continual presence of ACPC. The efficacy of the response was determined by comparison of steady-state current amplitudes to the same concentration pulse of NMDA in the continual presence of 10 μM glycine in the same cell. The efficacy of 10 μM ACPC relative to saturating glycine was 72.2 ± 2.2% (n = 5 cells) and 78.5 ± 1.0% (n = 3 cells) at 15 and 150 μM NMDA, respectively (Fig. 1C). Corresponding efficacies of 46.6 ± 7.2% (n = 5 cells) and 71.4 ± 3.7% (n = 3 cells), respectively, were obtained with 1 mM ACPC (Fig. 1C). Relative responses to the same concentrations of NMDA in the presence of ACPC in comparison to glycine controls measured at a holding potential of +60 mV were similar to relative responses measured at −60 mV (paired t test, $p > .4$ for 15 μM NMDA, n = 5 cells; $p > .9$ for 150 μM NMDA, n = 4 cells), indicating that ACPC efficacy is not voltage dependent.

This apparent difference in the efficacy of 1 mM ACPC warranted a more detailed examination of its concentration-effect relationship at both 15 and 150 μM NMDA. There was considerable overlap of the rising phases of both dose-response curves, with both curves reaching a plateau in efficacy between 5 and 250 μM ACPC, followed by a decrease in efficacy at concentrations of >250 μM (Fig. 2A). Increasing NMDA concentrations by 10-fold extended the plateau phase of the concentration-response curve and resulted in a smaller overall decrease in NMDA-mediated responses at millimolar concentrations of ACPC (Fig. 2A). Fitting this data to eq. 1 yielded a maximum efficacy ($E_{\max}$) of 72.8% in the presence of 15 μM NMDA and 82.9% in the presence of 150 μM. The concentration of half-maximal activation ($E_{1/2}$) by ACPC was 0.65 and 0.46 μM in the presence of 15 and 150 μM NMDA, respectively. The $I_{1/2}$ values deduced using eq. 1 were 2.0 mM in the presence of 15 μM NMDA and 10.7 mM in the presence of 150 μM NMDA.

The high concentrations of ACPC required to reduce its

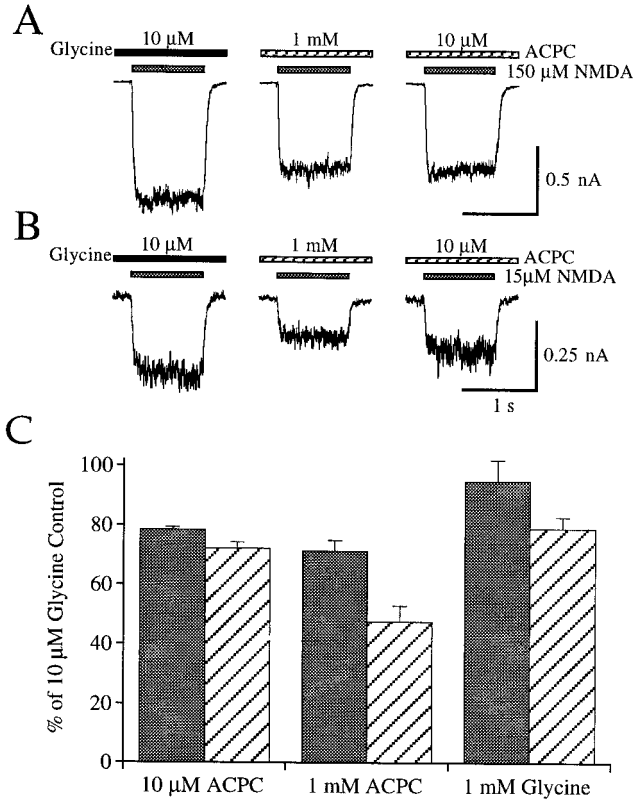

Fig. 1. Efficacy of 10 μM and 1 mM ACPC with 15 or 150 μM NMDA. A, representative records of currents elicited by a 1-s pulse of 150 μM NMDA (gray bars) in the continual presence of either 10 μM or 1 mM ACPC (striped bars) from cultured granule cells. The responses had steady-state amplitudes that were 73.2 and 72.1% of the control responses recorded in the continual presence of 10 μM glycine (black bar). B, when 15 μM NMDA was pulsed in the presence of either 10 μM or 1 mM ACPC, steady-state response amplitudes were 68.9 and 52.5% of the control responses recorded in the presence of 10 μM glycine. C, histogram showing a summary of comparisons exemplified in A and B for three to seven cells. In all cases, responses to ACPC were less than their glycine controls. In the presence of 15 μM NMDA (striped columns), relative responses to ACPC were reduced when the ACPC concentration was increased from 10 to 1000 μM, whereas in the presence of 150 μM NMDA (filled columns), relative responses were similar. Chloride channel currents elicited by 1 mM glycine alone were subtracted from responses to 1 mM glycine with either 15 or 150 μM NMDA and compared with NMDA-mediated responses in the presence of 10 μM glycine. These data indicate that 1 mM glycine can also change the efficacy of the response in an NMDA-dependent manner.

efficacy at low concentrations of NMDA (Fig. 2A) could possibly result from a high-affinity contaminating byproduct of ACPC synthesis rather than to ACPC itself. To investigate this possibility, experiments identical with those shown in Fig. 1 were repeated with three different lots of ACPC produced by different synthetic routes (Logusch, 1986; Vaidyanathan and Wilson, 1989; Schubert et al., 1990). The results obtained from each of these preparations were not significantly different from those presented in Fig. 1B (data not shown). Thus, it is highly unlikely that a low concentration of a putative high-affinity contaminant could produce the same relative partial agonism at 10 and 1000 μM ACPC for 15 μM NMDA for each of the three batches examined.

In the presence of 15 μM NMDA and 1 mM glycine, NMDA channel-mediated responses also had a reduced efficacy (78.9 ± 3.9%, n = 3 cells) in comparison with 10 μM glycine controls. Efficacy increased to 94.8 ± 7.2% (n = 4 cells) for responses measured in the presence of 150 μM NMDA and 1 mM glycine (Fig. 1C). Note that for 1 mM glycine responses, controls currents lacking NMDA had to be subtracted from those responses containing NMDA to remove the significant contribution resulting from glycine-gated chloride channels. Although the NMDA-dependent reduction in efficacy produced by 1 mM glycine is qualitatively similar to that of ACPC, different lots of glycine produced by different synthetic routes were not tested; thus, we cannot conclusively verify whether glycine or a contaminant is responsible for this action.

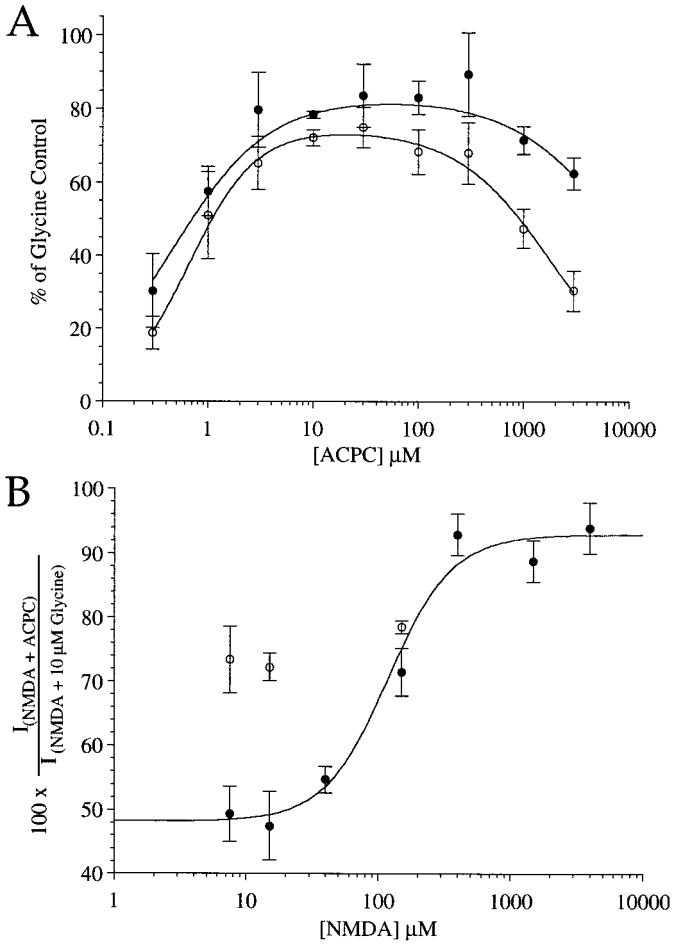

Fig. 2. Steady-state efficacy of ACPC varies with NMDA concentration in cultured cerebellar granule cells. A, ACPC concentration-response curves at 15 and 150 μM NMDA. Voltage-clamped cells where pulsed for 1 s with either 15 μM (○) or 150 μM NMDA (●) in the continual presence of varying concentrations of ACPC and compared with a control response in which the same concentration of NMDA was pulsed with 10 μM glycine. Data were fit with eq. 1. For 15 μM NMDA, E_{max} = 74.5%, $E_{1/2}$ = 0.65 μM, n_1 = 1.4, $I_{1/2}$ = 2.0 mM, and n_2 = 1.0 (n = 3–6 cells). For 150 μM NMDA, E_{max} = 83.1%, $E_{1/2}$ = 0.46 μM, n_1 = 1.0, $I_{1/2}$ = 10.7 mM, and n_2 = 0.8 (n = 3–7 cells). B, cells were pulsed for 1.5 s with NMDA (7.5 μM to 4 mM) in the continual presence of either 10 μM, 1 mM ACPC, or 10 μM glycine. ○, 10 μM ACPC responses relative to the 10 μM glycine control response with the same concentration of NMDA. ●, responses in the presence of 1 mM ACPC relative to the glycine control response. The solid line represents a fit using eq. 2. Final fit parameters were E_{max} = 92.9%, $E_{1/2}$ = 119.6 μM, and n_H = 1.8. For the fit, E_0 was held constant at 48.2% (n = 2–4 cells).

Data from Figs. 1 and 2 indicate a dependence of ACPC efficacy on NMDA concentration. A full NMDA concentration-response relationship for the efficacy of 1 mM ACPC is shown in Fig. 2B. When the data from Fig. 2B were fit with eq. 2, the maximal efficacy, E_{max}, at saturating concentrations of NMDA was 93%, whereas the minimal efficacy, E_0, of 1 mM ACPC at limiting concentrations of NMDA was 48.2%. The concentration of NMDA at which 1 mM ACPC increased by half its potential increase in efficacy, $E_{1/2}$, was 119 μM, and the slope of the concentration-response curve had a Hill coefficient (n_H) of 1.8. Note that a lower concentration of ACPC (10 μM) yields higher efficacies at 7.5, 15, and 150 μM (Fig. 2B).

NMDA concentration-response curves (3–300 μM) were acquired in the presence of either 10 μM glycine or 10 μM ACPC to determine whether ACPC differentially influences NMDA apparent affinity in comparison with glycine. ACPC (10 μM) was used because its responses with NMDA reside in the plateau phase of the ACPC concentration-response curves and because it is a 100-fold lower concentration than the concentration at which NMDA-dependent inhibition is observed (Fig. 2A), enabling maximal responses with minimal inhibitory effects. NMDA concentration-response measurements yielded an EC_{50} value of 36.0 ± 9.0 μM and a Hill coefficient of 1.5 ± 0.2 in the presence of ACPC (n = 4 cells) and an EC_{50} value of 35.2 ± 4.9 μM and Hill coefficient of 1.6 ± 0.2 in the presence of glycine (n = 4 cells, data not shown).

Cultured hippocampal neurons were selected for measuring the kinetics of onset and removal of ACPC to better define its actions on NMDA receptor channels (Fig. 3). Cultured hippocampal neurons have a high number of NMDA receptor channels relative to cerebellar granule cells and thus yield measurements with a better signal-to-noise ratio. It should be noted that relative steady-state current responses to 15 μM NMDA in the presence of either 10 μM or 1 mM ACPC recorded from hippocampal neurons were 71.9 ± 3.6 and 47.3 ± 5.2% of the responses to 15 μM NMDA and 10 μM glycine, respectively (n = 4 cells). These results were not significantly different from corresponding measurements of ACPC efficacy determined from cultured cerebellar granule cells (Fig. 1B).

Figure 3A illustrates the effects of a 2-s pulse of either 30 μM or 1 mM ACPC or of 10 μM glycine in the presence of 15 μM NMDA. Both 1 mM ACPC and 15 μM NMDA were chosen to minimize the efficacy of ACPC in comparison with glycine, so the kinetics of inhibition by ACPC could be easily observed. The application of NMDA alone produced currents in the absence of added coagonist (Fig. 3A), presumably due

to the presence of low concentrations of endogenous glycine in the hippocampal cultures. The average amplitude of these currents measured immediately before the application of a 1 mM pulse of ACPC was 7.8 ± 6.8% of the peak onset response to ACPC (n = 11 cells). The addition of exogenous glycine or ACPC caused a dramatic increase in NMDA receptor-mediated currents. When the responses shown in Fig. 3A are overlaid and enlarged (Fig. 3B), it can clearly be observed that the efficacy of the 30 μM ACPC response is relatively constant, whereas the efficacy of the 1 mM ACPC pulse changes significantly during the course of the ACPC pulse. The average peak activation in response to a pulse of 1 mM ACPC was 77.2 ± 5.3% (n = 10 cells) of peak activation in the presence of glycine (Fig. 3C). Although responses to glycine in the presence of NMDA decrease gradually to 86.8 ± 3.6% of the peak response for the length of the pulse (n = 10 cells), the response to 1 mM ACPC decreases rapidly to 61.9 ± 6.3% of its peak response with an exponential decay time constant of 33.4 ± 11.0 ms (n = 9 cells). Final steady-state responses to ACPC were 55.0 ± 3.2% of steady-state responses to glycine (Fig. 3C), consistent with the values obtained in Figs. 1 and 2. On removal of ACPC (1 mM), NMDA-mediated currents increased by 49 ± 4.9% compared with steady-state responses to ACPC (n = 7 cells). The efficacy of this peak response (peak offset, Fig. 3C) on removal of ACPC was 85.9 ± 6.4% of the steady-state response to the same concentration of NMDA in the presence of glycine (n = 10 cells). An identical experiment to that depicted in Fig. 3A was performed in the presence of 2 mM rather than 0.2 mM calcium to test the possibility that ACPC stimulatory or inhibitory effects might be different under more physiological conditions. Peak onset, peak offset, and steady-state responses to either 30 μM or 1 mM ACPC in the presence of 15 μM NMDA were similar to values reported above (n = 5 cells, data not shown).

Because glutamate is the physiological agonist that binds to the glutamate-binding site of the NMDA channel, ACPC concentration-response curves were measured with saturating (10 μM) glutamate. Under these conditions, the efficacy of ACPC ($\geq$1 μM) as a glycine-binding site agonist equals that of 10 μM glycine (Fig. 4A). The EC_{50} values for peak and steady-state responses to the application of 10 μM glutamate in the presence of varying concentrations of ACPC were 24.3 and 81.6 nM with Hill coefficients of 0.8 and 0.8, respectively (n = 3–5 cells, Fig. 4B). In the presence of ACPC, apparent dissociation of glutamate required two exponentials for successful fitting. τ_{fast} was 53.9 ± 8.8 ms (A_{fast} = 50.6 ± 5.4%) and τ_{slow} was 356.6 ± 39.6 ms (A_{slow} = 49.4 ± 5.4%, n = 8 cells), whereas the removal of glutamate in the presence of glycine yielded a τ_{fast} value of 96.9 ± 17.1 ms (A_{fast} = 46.7 ±

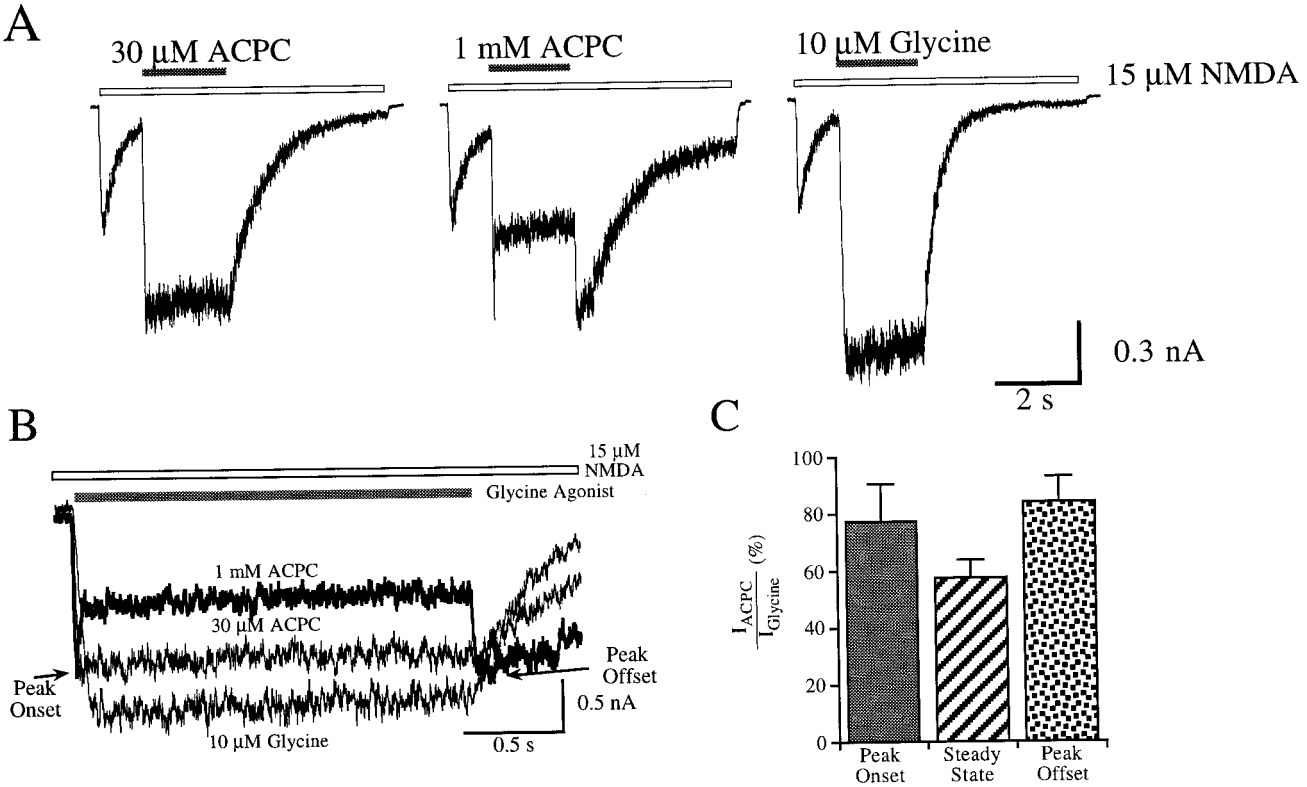

Fig. 3. Kinetics of ACPC association and dissociation in the presence of 15 μM NMDA. A, a cultured hippocampal neuron was bathed with 15 μM NMDA in the presence of endogenous glycine. After 1.5 s, either 30 μM or 1 mM ACPC or 10 μM glycine was added for 2 s. Exogenous glycine agonist was then removed, followed by NMDA removal 3.5 s later. Traces depicted are from the same neuron. The addition of 30 μM or 1 mM ACPC caused a rapid rise in inward current that had a peak amplitude of 86% in comparison to the glycine control peak amplitude. ACPC (1 mM) responses then rapidly decayed to 50.4% of the control steady-state current, whereas responses to 30 μM ACPC only decreased slightly to 80.4% of control responses. Removal of 1 mM ACPC caused a transient increase in inward current to 93.3% of the glycine steady-state current before a slow current decay (middle), whereas the removal of 30 μM ACPC (left) or 10 μM glycine (right) did not yield this peak offset response. B, enlargement and overlay of onset and removal glycine agonist in A emphasized the differences in onset and removal kinetics of ACPC and glycine. Only the 1 mM ACPC pulse trace (thick lines) yielded the complex kinetics of the peak onset and peak offset responses. C, comparison of the relative amplitudes on the addition and removal of 1 mM ACPC indicates that the efficacy of ACPC in comparison with glycine in the presence of 15 μM NMDA is significantly increased at peak onset and peak offset amplitudes.

4.7%) and a τ_{slow} value of 525.5 ± 94.1 ms (A_{slow} = 53.3 ± 4.7%, n = 8 cells).

Glutamate concentrations were lowered to a concentration comparable to 15 μM NMDA (1.0 μM glutamate), and hippocampal neurons were pulsed with 10 μM glycine or 3 mM ACPC (Fig. 5A). In the continual presence of 1 μM glutamate, peak responses to pulses of ACPC could be differentiated from steady-state responses at concentrations of >1 μM ACPC. Peak responses approached values comparable to the control glycine peak at 100 μM ACPC (96.8 ± 9.7%) and exceeded (112.7 ± 4.5%) the glycine peak response at 3 mM ACPC (Fig. 6A). Fits to eq. 3 yielded an EC_{50} value of 0.7 μM and an n_H value of 0.7. In contrast, steady-state responses over the same concentration range decreased with increasing ACPC concentration. Fits to eq. 4 yielded an IC_{50} value of 3.3 mM and an n_H value of 0.8 (Fig. 6A, n = 3–5 cells). Interestingly, when ACPC concentration-response analysis is compared between the peak response in 1 μM glutamate shown in Fig. 6A and the steady-state response to a 10 μM pulse of glutamate in various concentrations of ACPC (Fig. 4B), ACPC EC_{50} values decrease by 8.7-fold with a 10-fold increase in glutamate concentration (Fig. 6C).

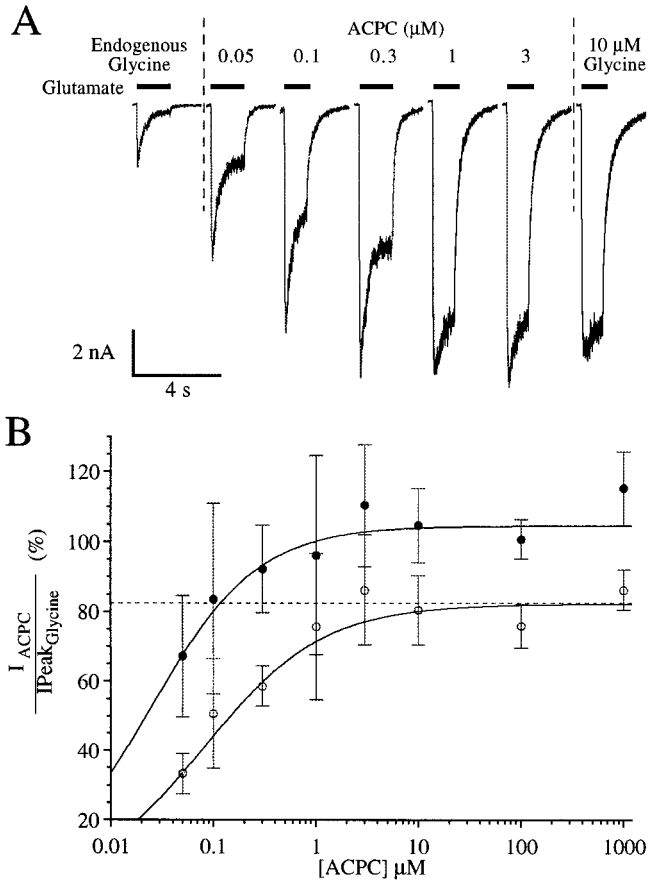

Fig. 4. ACPC is fully efficacious in the presence of 10 μM glutamate. A, cultured hippocampal neurons were pulsed with 10 μM glutamate in the presence of either 50 nM to 3 μM ACPC, 10 μM glycine, or solutions containing no added glycine (endogenous glycine). Inward currents peaked and desensitized to steady-state levels in a manner dependent on ACPC concentration. Above 100 nM ACPC, peak responses slightly exceeded peak responses to glutamate in the presence of glycine. No difference was observed in steady-state amplitudes for responses elicited in the presence of 1 or 3 μM ACPC in comparison with those elicited in the presence of 10 μM glycine. The decay of the responses on the removal of glutamate in the presence of either ACPC or glycine had kinetics that required two exponential fits (see *Results*). B, peak (●) and steady-state (○) concentration-response analysis of NMDA receptor-mediated currents elicited in the presence of 50 nM to 1 mM ACPC in comparison with peak currents elicited in the presence of 10 μM glycine. Responses of 30 nM ACPC were not included in this analysis because they were similar to responses elicited in the absence of any added glycine agonist. Dotted line indicates the relative amplitude of steady-state responses to 10 μM glutamate and 10 μM glycine in comparison to their peak responses. Solid lines represent fits to the eq. 3. Fitted parameters for peak measurements were I_{max} = 104.6%, EC_{50} = 24.3 nM, and n_H = 0.8. For steady-state measurements, fitted parameters were I_{max} = 82.3%, EC_{50} = 81.6 nM, and n_H = 0.8.

Figure 5, A and B, indicate that responses to the glycine control pulse in the presence of 1 μM glutamate desensitized significantly, yielding a steady-state response that was 69.6 ± 4.5% of its peak response (Fig. 6A). The peak response to a 1 mM ACPC pulse equaled the glycine peak response (100.9 ± 2.5%, n = 5 cells) but decayed to a lower steady-state level that was 59.1 ± 6.8% of the glycine steady-state response. Figure 6B shows that the ratio between the steady-state and peak response to ACPC decreases with increasing ACPC concentration, with a half-maximal inhibition of 1.3 mM and Hill coefficient of 0.7 (n = 5 cells). At low concentrations of ACPC, this ratio approaches the ratio of the 10 μM glycine control and is a measure of the degree of glycine-insensitive desensitization (Villarroel et al., 1998) under these conditions. The time constant of decay from peak to steady state of NMDA channel currents activated with a pulse of 10 μM glycine was 202.6 ± 32.5 ms (Fig. 5C, n = 15 cells). Responses in the presence of 1 mM ACPC also decayed with a similar time constant (211.4 ± 24.5 ms, n = 5 cells).

In the presence of either 15 μM NMDA or 1 μM glutamate, the removal of ACPC concentrations of >300 μM yielded an initial rapid increase in inward current followed by a slow decrease in current (Figs. 3, A and B, and 5, A and D). Biphasic exponential fits of currents during the removal of ACPC in the presence of 15 μM NMDA yielded an average time constant of 32.2 ± 6.5 ms for the rising phase and a time constant of 1812.0 ± 837.6 ms for the declining phase of the response (n = 9 cells). In the presence of 1 μM glutamate (Fig. 5D), no significant change in either the rising or declining phase time constants was found for increasing concentrations of ACPC from 300 μM to 3 mM. The average time constants for the rising and declining phases of the response to the removal of 0.3 to 3 mM ACPC were 125.8 ± 52.4 and 1579.2 ± 463.6 ms, respectively (n = 6 cells, Fig. 5E). No rise in inward current was observed on the removal of ACPC concentrations of <300 μM; the time course of the decay of current could be characterized by a single exponential time constant of 852.4 ± 159.7 ms in the presence of 15 μM NMDA and 766.2 ± 97.9 ms in the presence 1 μM glutamate. In experiments on the same cells, the removal of 10 μM glycine caused a reduction of inward current with a time constant of 542.2 ± 77.4 ms in the presence of 1 μM glutamate (n = 16 cells) and 420.9 ± 43.9 ms in the presence of 15 μM NMDA (n = 10 cells). It should be noted that the NMDA agonist was removed before complete deactivation after the removal of ACPC to prevent excessive current rundown resulting from prolonged agonist applications.

The complexity of activation and modulation of NMDA channels coupled with the evidence that ACPC acts at both glutamate- and glycine-binding sites indicated that standard concentration-response analysis may not accurately predict ACPC action (see *Discussion*). We therefore tried to simulate

the ACPC data presented (Figs. 4–6) with the model shown schematically in Fig. 7A. This model is based on a model presented previously (Benveniste et al., 1990), in which there are two binding sites for both glutamate and glycine and an element of negative cooperativity for agonist binding. Glutamate is used as the glutamate agonist, ACPC is used as the glycine agonist, and additional states have been added to provide full two-site competitive antagonism. The forward and reverse rate constants are presented in Table 1.

Selected simulated data of a glycine agonist pulse in the

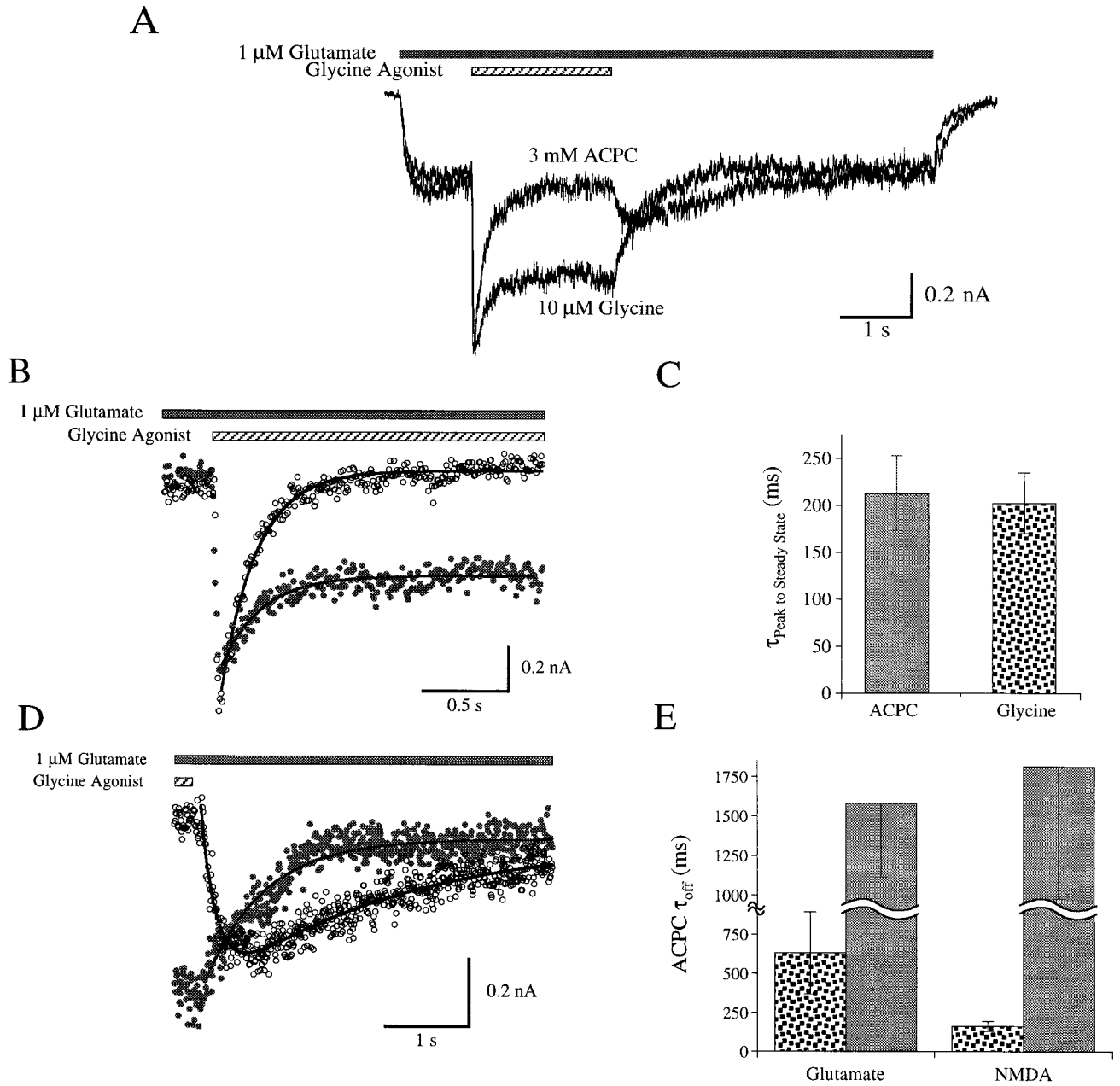

Fig. 5. Kinetics of ACPC association and dissociation in the presence of 1 μM glutamate. ACPC (3 mM) or glycine (10 μM) pulsed in the presence of 1 μM glutamate and resulting NMDA channel-mediated responses were recorded from cultured hippocampal neurons. A, on the addition of 1 μM glutamate, a significant degree of inward current was observed resulting from NMDA channel activation by glutamate with endogenous glycine. On the addition of either ACPC or glycine, inward current rapidly increased, peaked, and then decreased to a steady-state level. Although peak currents elicited by the 3 mM ACPC pulse were 113% of the peak currents elicited by glycine in this cell, steady-state currents in the presence of 3 mM ACPC were 36.8% of the steady-state current elicited by glutamate and 10 μM glycine. Peak offset responses on removal of 3 mM ACPC were 87.8% of the steady-state glycine control responses. B, peak to steady-state decays during a pulse of either 10 μM glycine (●) or 3 mM ACPC (○) were fitted with single exponentials and yielded time constants of 228 and 204 ms, respectively. C, bar graph of peak to steady-state decay time constants. No significant difference is observed between 3 mM ACPC (filled column) and 10 μM glycine (speckled column) in the presence of 1 μM glutamate. D, fit to responses of the removal of 3 mM ACPC (○) requires the sum of two exponentials. The fast time constant of 183 ms describes the rise to the peak offset response, whereas the slow time constant of 2169 ms describes the decay of the response. Note that the removal of 10 μM glycine in the presence of glutamate can be fit by a single exponential time constant of 690 ms. E, comparison of the rising (speckled column) and declining (filled column) phase components time constants during the removal of 1 mM ACPC in the presence of either 15 μM NMDA or 1 μM glutamate. The time constant of the rising phase after the removal of ACPC in the presence of 15 μM NMDA is ~ 4-fold faster than that in the presence of 1 μM glutamate. In contrast, the declining phases decay with similar time courses. The gap indicates a change in scale of the bar graph.

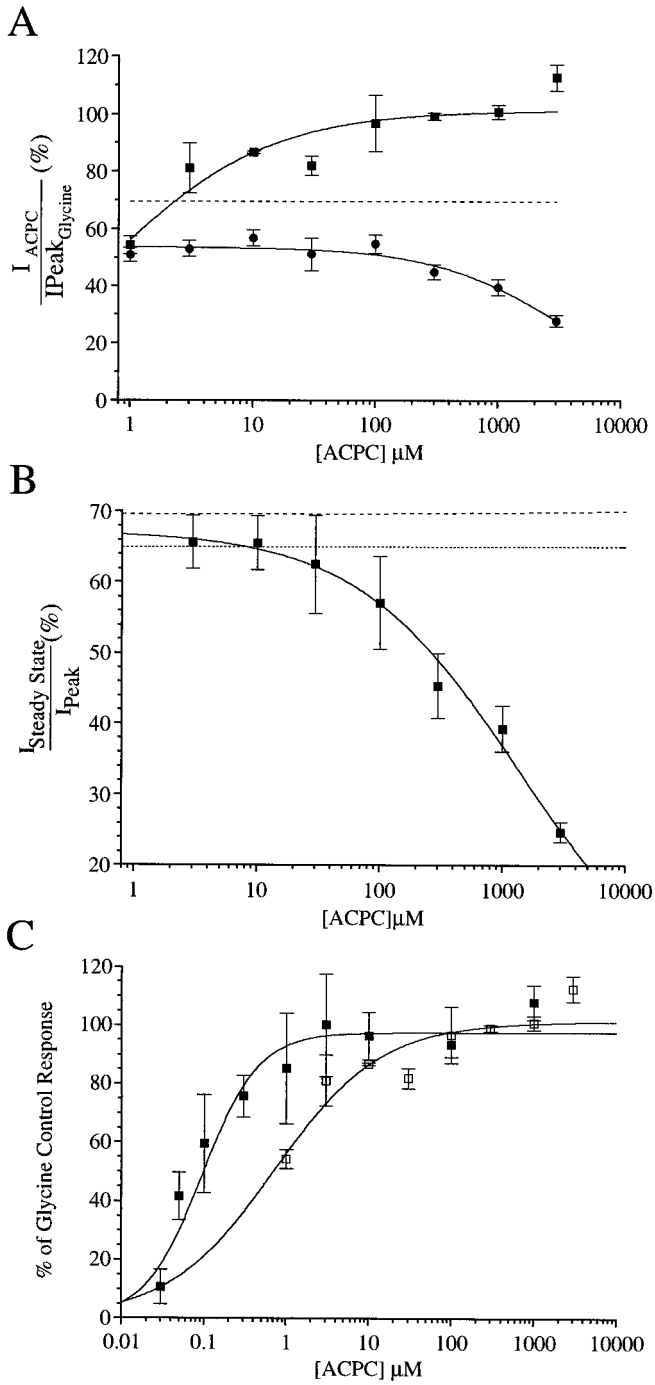

Fig. 6. ACPC apparent affinities and efficacies in the presence of 1 μM glutamate. A, peak amplitudes (■) and steady-state amplitudes (●) to a pulse of varying concentrations of ACPC (1 μM to 3 mM) in the presence of 1 μM glutamate were plotted relative to the peak response elicited by 10 μM glycine under similar conditions. Peak responses were fit according to eq. 3 and yielded an I_{max} value of 101.3%, an EC_{50} value of 0.71 μM, and an n_H value of 0.7. Steady-state responses were fit according to eq. 4 and yielded an I_{max} value of 53.8%, an IC_{50} value of 3.27 mM, and an n_H value of 0.8. Dashed line indicates the steady-state amplitude to the 10 μM glycine control response in the presence of 1 μM glutamate. B, ratio of the steady-state to peak response for differing concentrations of ACPC according to the protocol for the experiment shown in Fig. 5A. Fits to eq. 4 yielded an I_{max} value of 67.3%, an IC_{50} value of 1.34 mM, and an n_H value 0.7. Dashed line indicates the steady-state to peak ratio for the glycine control response. Dotted line represents the standard deviation of that response. C, Comparison of the steady-state response to 10 μM glutamate in the presence of varying concentrations of ACPC (Fig. 4B, ■) to peak responses to varying concentrations of ACPC in the presence of 1 μM glutamate (Fig. 6A, □). Responses are represented as percentages of their glycine control response and emphasize the 8.7-fold difference in apparent affinity of ACPC in each condition.

presence of 1 μM glutamate are presented in Fig. 7B. This figure indicates that onset responses to 3 mM ACPC produced the characteristic peak to steady-state decay that had been observed in Fig. 5, A and B. The peak to steady-state decay time constant of the response to 10 μM or 3 mM ACPC simulated from our model was 131 and 146 ms and is comparable to the 205-ms decay time constant resulting from a simulated 10 μM glycine pulse. Furthermore, biphasic offset responses (Fig. 5, D and E) to the removal of ACPC were also observed (Fig. 7B). Kinetics observed on the removal of 3 mM ACPC were 107 ms for the rising phase and 1738 ms for the declining phase.

Concentration-response simulations (Fig. 7C) over the same range of ACPC concentrations presented in Fig. 6A appeared similar to the experimental data. Analysis of the peak current according to eq. 3 yielded an EC_{50} value of 0.9 μM and a Hill coefficient of 0.8. Steady-state inhibition like that observed in the experimental data (Fig. 6, A and B) was also exhibited by this model (Fig. 7, C and D). Steady-state responses at relatively low ACPC concentrations (E_0) reached 61% of the modeled peak glycine response with an IC_{50} value of 2.7 mM (Fig. 7C). In Fig. 7D, the ratio of steady-state to peak measurements for the experimental data almost completely overlays the values predicted by this model. Simulated peak and steady-state responses to pulses of 10 μM glutamate in the presence of differing concentrations of ACPC also approximated experimental results (Fig. 4B). Peak dose-response analysis yielded EC_{50} and I_{max} values of values of 13.3 nM and 97.5% with an n_H value of 0.9, whereas analysis of steady-state responses yielded EC_{50} and I_{max} values of 49.9 nM and 86.8% with an n_H value of 0.9.

These simulations predict that steady-state apparent affinities for glutamate deduced from glutamate concentration-response curves will be shifted slightly in the presence of 10 μM ACPC (EC_{50} = 1.1 μM) in comparison to similar curves generated with kinetic parameters for glycine (EC_{50} = 0.6 μM). Such differences might not be detectable under our experimental conditions.

One-site models for NMDA channel activation like that shown in Scheme 2 exhibited the same basic characteristics observed for the two-site model (Fig. 7B). The main difference between one- and two-site models is that one-site models did not have a prolonged plateau phase of lower efficacy in comparison with glycine controls but rather increased, peaked, and declined over a narrower range of ACPC concentrations.

The contribution of endogenous glycine has been ignored in these simulations. Such a contribution should affect the rising phase of the ACPC concentration-response curve. At very low ACPC concentrations, the NMDA channel activity will be abnormally high. As ACPC concentration increases, the probability that ACPC will replace glycine as the agonist bound at the glycine-binding site will also increase. This may partially explain the low Hill coefficient observed in the experimental data for the rising phase of the ACPC concentration-response curve (Fig. 2A). In contrast, because the ACPC inhibitory effect probably results from the binding of ACPC at the glutamate agonist-binding site, endogenous glycine will not affect the degree of inhibition observed. For this reason, the

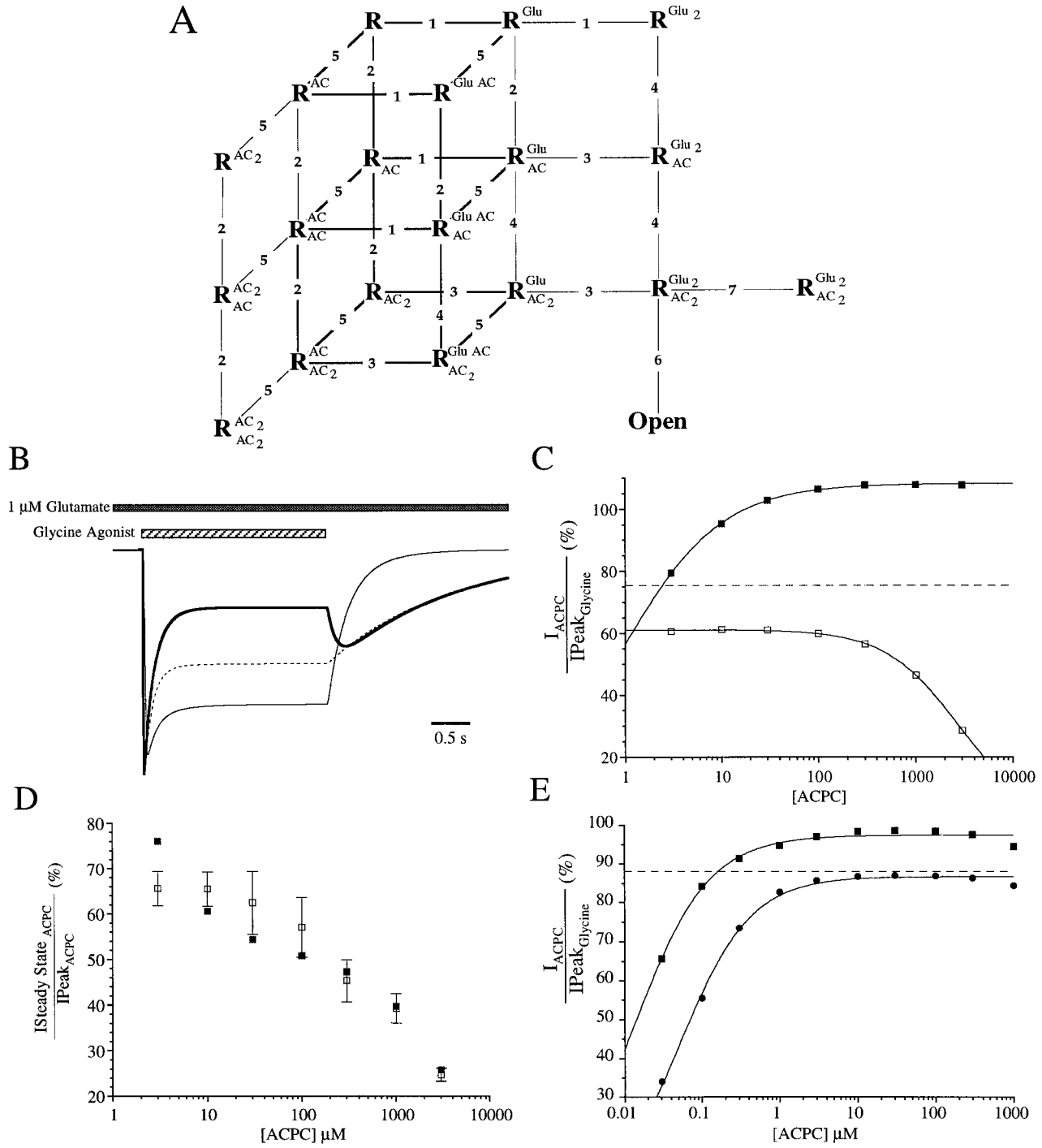

Fig. 7. Simulations of ACPC responses in the presence of glutamate as a glycine-site agonist and a glutamate-site competitive antagonist. A, model in which NMDA channel activation requires the binding of two agonist molecules at the glutamate-binding site and two agonist molecules at the glycine-binding site and includes competitive antagonism at the glutamate-binding site. In addition, an explicit transition was modeled between the fully liganded closed and open states (transition 6). Note that an additional transition to another fully liganded closed state has been modeled to simulate glycine-insensitive desensitization (transition 7). Superscripts indicate the molecules that bind to the glutamate-binding site; subscripts indicate the molecules that bind to the glycine-binding site. Forward and reverse transition rate constants are given in Table 1. B, results from the model depicted in A for a protocol similar to that used in Fig. 5A. Thin line represents the response to 10 μM glycine in the presence of 1 μM glutamate; dashed and thick lines represent the response to 10 μM and 3 mM ACPC, respectively. C, concentration-response analysis of simulated peak and steady-state responses like those in B. For peak responses (■), I_{max} = 108.3%, EC_{50} = 0.9 μM, and n_H = 0.8. For steady-state responses (□), I_{max} = 61.3%, IC_{50} = 2.67 mM, and n_H = 1.2. Horizontal line indicates the steady-state response to 10 μM glycine. All responses are relative to the 10 μM glycine peak response. D, comparison of steady-state to peak amplitude ratios for experimental data (Fig. 6B) to simulated data. □, experimental data. ■, simulated data. E, comparison of simulated peak (■) and steady-state responses (●) to 10 μM glutamate pulses in the presence of various concentrations of ACPC. Responses are relative to peak amplitudes for responses simulated for 10 μM glutamate and 10 μM glycine control response. Fits of concentration-response data for peak responses yielded an I_{max} value of 97.5%, an EC_{50} value of 13.3 nM, and an n_H value of 0.9, whereas fits of ACPC and 10 μM glutamate steady-state responses yielded an I_{max} value of 86.8%, an EC_{50} value of 49.9 nM, and an n_H value of 0.9. Dashed line indicates the simulated steady-state amplitude of the glycine control response relative to its peak amplitude.

response to glutamate in the absence of added ACPC was not subtracted from the measured responses.

Discussion

For ligand-gated ion channels, partial agonists are commonly thought to have a reduced efficiency of causing an allosteric transition (*) between a channel in an agonist bound closed state (RA) and its open state (RA_{open}) relative to full agonists:

$$R + A \rightleftharpoons RA \overset{*}{\rightleftharpoons} RA_{Open}$$

Scheme 1.

Apparent partial agonism could also be observed if the agonist (A) increased channel transitions to other agonist-bound nonconducting (desensitized) states or if an agonist could not saturate its respective binding site to yield a fully efficacious response because of experimental limitations (e.g., lack of solubility).

Because NMDA receptor ion channels require the binding of two coagonists, glutamate and glycine, for channel activation (Kleckner and Dingledine, 1988), a putative partial agonist could act as a full agonist at one binding site but also reduce the binding of agonist at the other type of coagonist binding site (e.g., Scheme 2).

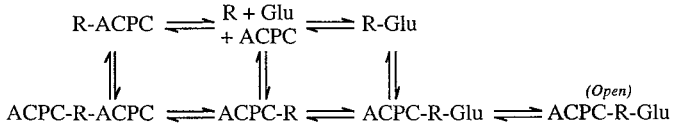

Scheme 2.

ACPC Apparently Acts at Both Glycine- and Glutamate-Binding Sites

Evidence presented here indicates that ACPC acts as a full glycine agonist. In the absence of added glycine, increasing concentrations of ACPC up to 10 μM yields an increase in NMDA receptor-mediated responses (Figs. 2A and 4A). In addition, with saturating glutamate concentrations, ACPC can attain 100% efficacy (Fig. 4B).

TABLE 1
Rate constants for simulated data of ACPC as a full glycine-site agonist and glutamate-site competitive antagonist

Transition[a]	Drug	Binding Site	k_{on}	k_{off}
			$\mu M^{-1}\ s^{-1}$	s^{-1}
ACPC				
1	Glutamate	Glutamate	6.0	0.6
2	ACPC	Glycine	10.0	0.06
3	Glutamate	Glutamate	6.0	4.0
4	ACPC	Glycine	10.0	0.4
5	ACPC	Glutamate	1.0	2500
Glycine control				
1	Glutamate	Glutamate	6.0	0.60
2	Glycine	Glycine	10.0	0.65
3	Glutamate	Glutamate	6.0	2.30
4	Glycine	Glycine	10.0	2.12
Both				
6			100[b]	300
7			0.5[b]	2.0

[a] Transition numbers are according to the scheme depicted in Fig. 7A.
[b] Indicates that units are s^{-1}.

The action of ACPC as a low-affinity glutamate-site competitive antagonist is indicated by an increase in the steady-state responses (relative to 10 μM glycine) to millimolar concentrations of ACPC with increasing concentrations of NMDA (Figs. 1 and 2) or glutamate (Figs. 4B and 6A).

The actions of ACPC as a glycine-site agonist and glutamate-site competitive antagonist can be kinetically isolated by applying high concentrations of ACPC in the presence of a subsaturating concentration of glutamate agonist (Figs. 3A and 5A). Peak onset responses to a pulse of 1 or 3 mM ACPC can reach 100% efficacy (Figs. 6A and 7A), reaffirming the role of ACPC as a full glycine agonist. At these ACPC concentrations, the time course of current decays from peak to steady state should be limited by glutamate agonist dissociation if steady-state currents contain a component resulting from competitive antagonism by ACPC at the glutamate-binding site (Scheme 2). A 1 mM ACPC pulse in the presence of 15 μM NMDA resulted in a peak to steady-state decay time constant that was similar to the apparent dissociation time constant observed on removal of NMDA in the presence of ACPC (27.8 $\pm$ 7.6 ms, n = 5 cells, data not shown). In addition, the peak to steady-state decay time constant for a pulse of 1 or 3 mM ACPC in the presence of 1 μM glutamate (Fig. 5, B and C) was similar to the weighted average of the two exponential apparent dissociation time constant (204.1 $\pm$ 30.9 ms, n = 8 cells) observed on the removal of glutamate in the presence of ACPC (Fig. 4A). However, it should be noted that control glycine responses in the presence of glutamate decay with a similar time course (Fig. 5C). This might suggest that other NMDA receptor channel desensitization phenomena (e.g., glutamate-sensitive desensitization) are predominant when a subsaturating concentration of glutamate is used (Nahum-Levy and Benveniste, in preparation).

The biphasic response observed on removal of ACPC in the presence of glutamate or NMDA also indicates that ACPC acts as both a glycine agonist and a glutamate competitive antagonist (Figs. 3A and 6A). The rising phase of the peak offset response probably results from glutamate agonist rebinding after rapid, low-affinity dissociation of ACPC, whereas the declining phase will mainly depend on high-affinity, slow dissociation of ACPC from its glycine-binding site.

Additional Mechanisms Contributing to Putative Partial Agonism of ACPC

According to Fig. 2A, there is a >2000-fold difference between $E_{1/2}$ and $I_{1/2}$ values for ACPC. Standard dose-response analysis (e.g., eqs. 3 and 4, I_{max} = 1) with such a difference between EC_{50} and IC_{50} values would predict that an intermediate ACPC concentration could be found that would yield a 100% efficacious response in comparison with the glycine control. Because this was not observed experimentally, we attempted to find an additional mechanism that could potentially account for a reduced ACPC efficacy at relatively low ACPC concentrations. Such a mechanism must fulfill the following criteria: 1) the mechanism must be dependent on glutamate agonist concentration, because increasing glutamate agonist concentrations to supersaturating levels yields full agonism (Figs. 2B and 4A), and 2) the mechanism must yield fully efficacious peak onset responses to a pulse of high concentrations of ACPC (>100 μM) in the presence of 1 μM

glutamate but decay to less efficacious steady-state responses in comparison with glycine (Fig. 5, A and B).

Simple mechanisms by which bound ACPC constitutively reduces the efficiency of NMDA channel opening by modifying transitions between open and closed states (Scheme 1) can be discounted, because such a mechanism would not cause efficacy changes during a pulse of ACPC (criterion 2, above).

A mechanism whereby glycine and ACPC would differentially affect glutamate agonist affinity would fulfill both of the above criteria; however, no significant differences in EC_{50} values and Hill coefficients were determined for NMDA concentration-response analysis performed in the presence of 10 μM ACPC or glycine.

Simple dose-response analysis that would predict that a fully efficacious response be found at an intermediate ACPC concentration is based on assumptions of a single-binding site model. However, activation of the NMDA receptor channel probably requires the binding of two molecules of glutamate agonist and two molecules of glycine agonist (Benveniste and Mayer, 1991; Clements and Westbrook, 1991) and, changes in agonist apparent affinity probably occur during the activation process (Benveniste et al., 1990; R. Nahum-Levy and M. Benveniste, in preparation). These factors may invalidate the interpretation of simplistic dose-response analysis.

Indeed, with the model depicted in Fig. 7A, simulated responses to a pulse of relatively high concentrations of ACPC in the presence of 1 μM glutamate had peak to steady-state decays and biphasic offset decays (Fig. 7B) that were similar to experimental data (Fig. 5A). In addition, comparison of Fig. 6A with Fig. 7C indicated that the model could also predict the concomitant increase in the peak response with a decrease in the steady-state response with increasing ACPC concentrations, and concentration analysis of steady-state to peak ratios virtually overlapped experimental data (Fig. 7D). Figure 7E indicates that the model also predicts that ACPC will be fully efficacious under conditions of saturating glutamate with EC_{50} and I_{max} values for ACPC-simulated peak and steady state responses within 2-fold of experimental data (Fig. 4B). This combined evidence suggests that ACPC putative partial agonism can be explained solely by its concurrent action as a high-affinity glycine-site full agonist and a low-affinity glutamate-site competitive antagonist.

Physiological Implications

Figure 4, A and B, indicates that 1 mM ACPC acts as a full agonist in the presence of saturating concentrations of glutamate (10 μM), yet the acute administration of ACPC has been shown to be neuroprotective (Long and Skolnick, 1994; Fossom et al., 1995b). Thus, either ACPC causes neuroprotection in vivo via a mechanism unrelated to NMDA receptor ion channels, or the concentration of glutamate that causes neurotoxicity as a result of ischemic insult is quite low.

In the rat, a 300 mg/kg dose of ACPC yields plasma concentrations of ~5 mM (Cherkofsky, 1995) without toxic effects (Fossom et al., 1995b); therefore, ACPC concentrations in the brain could reach a several millimolar concentration. For millimolar concentrations of ACPC, a simple type of competitive inhibition might be used to estimate the ratio of the NMDA channel response to glutamate and ACPC in comparison with glutamate and glycine:

$$\frac{I_{\text{glutamate + ACPC}}}{I_{\text{glutamate + glycine}}} = \frac{1 + \dfrac{K_d}{[\text{glutamate}]}}{\dfrac{K_d}{[\text{glutamate}]}\left(1 + \dfrac{[\text{ACPC}]}{K_i}\right) + 1} \quad (5)$$

Assuming an apparent equilibrium dissociation constant (K_d) for glutamate binding to be 2.3 μM (Patneau and Mayer, 1990) and an equilibrium dissociation constant for ACPC at the glutamate-binding site (K_i) of 2 mM, then 3.5 μM glutamate and 5 mM ACPC would yield a response that would be 50% of the response of the same concentration of glutamate in saturating glycine.

During ischemic insult, glutamate concentrations can reach 30 μM (Benveniste et al., 1984; Globus et al., 1991). However, on recirculation after ischemic insult, glutamate levels fall rapidly to ~4 μM but require ~ 20 to 30 min to return to baseline glutamate levels. According to eq. 5, the degree of the NMDA receptor channel immediate and delayed response in the presence of 5 mM ACPC would be reduced by 15 and 48% for 30 and 4 μM glutamate, respectively.

Because ACPC and other NMDA antagonists can cause significant neuroprotection when administered up to several hours after ischemic insult (Hartley and Choi, 1989; Fossom et al., 1995b), the trigger for glutamate-induced neurotoxicity may be micromolar levels of glutamate for a sustained time period rather than higher concentrations of glutamate for a brief time. If this is true, then the hypothesis that "ACPC-like" putative partial agonists may prevent neurotoxicity without serious side effects could be rationalized. Normal synaptic transmission is characterized by a high concentration of glutamate (~1 mM) for a brief time period (~1 ms) (Clements et al., 1992). Under such conditions, 5 mM ACPC would inhibit the response to 1 mM glutamate by <1%. Thus, synaptic activation of NMDA receptors would not be impaired and would possibly limit psychotomimetic side effects. However, if under pathological conditions the concentration of glutamate are sustained in the low micromolar range, ACPC could yield substantial protection against glutamate induced neurotoxicity.

Acknowledgments

The authors would like to thank Sara Shavit for preparation of the hippocampal cultures and expert technical assistance.

References

Benveniste H, Drejer J, Schousboe A and Diemer NH (1984) Elevation of the extracellular concentrations of glutamate and aspartate in rat hippocampus during transient cerebral ischemia monitored by intracerebral microdialysis. *J Neurochem* **43:**1369–1374.

Benveniste M, Clements JD, Vyklicky L Jr and Mayer ML (1990) A kinetic analysis of the modulation of N-methyl-D-aspartic acid receptors by glycine in mouse cultured hippocampal neurones. *J Physiol (Lond)* **428:**333–357.

Benveniste M and Mayer ML (1991) Kinetic analysis of antagonist action at N-methyl-D-aspartic acid receptors: Two binding sites each for glutamate and glycine. *Biophys J* **59:**560–573.

Bigge CF and Boxer PA (1994) Neuronal cell death and strategies for neuroprotection. *Ann Rep Med Chem* **29:**13–21.

Boje KM, Wong G and Skolnick P (1993) Desensitization of the NMDA receptor complex by glycinergic ligands in cerebellar granule cell cultures. *Brain Res* **603:**207–214.

Cherkofsky SC (1995) 1-Aminocyclopropanecarboxylic acid: Mouse to man interspecies pharmacokinetic comparisons and allometric relationships. *J Pharm Sci* **84:** 1231–1235.

Choi DW (1992) Excitotoxic cell death. *J Neurobiol* **23:**1261–1276.
Clements JD, Lester RAJ, Tong G, Jahr CE and Westbrook GL (1992) The time course of glutamate in the synaptic cleft. *Science (Wash DC)* **258:**1497–1150.
Clements JD and Westbrook GL (1991) Activation kinetics reveal the number of glutamate and glycine binding sites on the N-methyl-D-aspartate receptor. *Neuron* **7:**605–613.
Fossom LH, Basile AS and Skolnick P (1995a) Sustained exposure to 1-aminocyclopropanecarboxylic acid, a glycine partial agonist, alters *N*-methyl-D-aspartate receptor function and subunit composition. *Mol Pharmacol* **48:**981–987.
Fossom LH, Von Lubitz DKJE, Lin RC-S and Skolnick P (1995b) Neuroprotective actions of 1-aminocyclopropanecarboxylic acid, a partial agonist at strychnine-insensitive glycine sites. *Neurol Res* **17:**265:-269.
Gallo V, Ciotti MT, Coletti A, Aloisi F and Levi G (1982) Selective release of glutamate from cerebellar granule cells differentiating in culture. *Proc Natl Acad Sci USA* **79:**7919–7923.
Garthwaite G and Garthwaite J (1986) Neurotoxicity of excitatory amino acid receptor agonists in rat cerebellar slices: Dependence on calcium concentration. *Neurosci Lett* **66:**193–198.
Globus MY-T, Busto R, Martinez E, Valdés I, Dietrich WD and Ginzberg MD (1991) Comparative effect of transient global ischemia on extracellular levels of glutamate, glycine, and γ-aminobutyric acid in vulnerable and nonvulnerable brain regions in the rat. *J Neurochem* **57:**470–478.
Hartley DM and Choi DW (1989) Delayed rescue of N-methyl-D-aspartate receptor mediated neuronal injury in cortical culture. *J Pharmacol Exl Ther* **250:**752–758.
Johnson JW and Ascher P (1987) Glycine potentiates the NMDA response in cultured mouse brain neurons. *Nature (Lond)* **325:**529–531.
Kleckner NW and Dingledine R (1988) Requirement for glycine inactivation of NMDA-receptors expressed in *Xenopus* oocytes. *Science (Wash DC)* **241:**835–837.
Logusch EW (1986) Facile synthesis of D,L-phosphinothricin from methyl 4-bromo-2-phthalimidobutyrate. *Tetrahed Lett* **27:**5935–5939.
Long JB and Skolnick P (1994) 1-Aminocyclopropanecarboxylic acid protects against dynorphin A-induced spinal injury. *Eur J Pharmacol* **261:**295–301.
Maccecchini ML (1995) Partial agonism and neuroprotection, in *Ischemic Stroke: Recent Advances in Understanding and Therapy* (Grotta J, Miller LP and Buchan AM eds) pp 140–168, International Business Communications, Southboro.
Mayer ML and Westbrook GL (1987) Permeation and block of N-methyl-D-aspartic acid receptor channels by divalent cations in mouse cultured central neurones. *J Physiol (Lond)* **394:**501–527.
McBain CJ, Kleckner NW, Wyrick S and Dingledine R (1989) Structural requirements for activation of the glycine co-agonist site of *N*-methyl-D-aspartate receptors expressed in *Xenopus* oocytes. *Mol Pharmacol* **36:**556–565.
Meldrum B (1994) Neuroprotection by NMDA and non-NMDA glutamate antagonists, in *Direct and Allosteric Control of Glutamate Receptors* (Palfreyman MG, Reynolds IJ and Skolnick P eds) pp 127–138, CRC Press, Boca Raton.
Muir KW, Grosset DG, Gamzu E and Lees KR (1994) Pharmacological effects of the non-competitive NMDA antagonist CNS 1102 in normal volunteers. *Br J Clin Pharmacol* **38:**33–38.
Parsons CG, Quack G, Bresink I, Baran L, Przegalinski E, Kostowski W, Krzascik P, Hartmann S and Danysz W (1995) Comparison of the potency, kinetics and voltage-dependency of a series of uncompetitive NMDA receptor antagonists in vitro with anticonvulsive and motor impairment activity *in vivo*. *Neuropharmacology* **34:**1239–1258.
Patneau DK and Mayer ML (1990) Structure-activity relationships for amino acid transmitter candidates acting a N-methyl-D-aspartate and quisqualate receptors. *J Neurosci* **10:**2385–2399.
Priestley T and Kemp JA (1994) Kinetic study of the interactions between the glutamate and glycine recognition sites on the N-methyl-D-aspartic acid receptor complex. *Mol Pharmacol* **46:**1191–1196.
Rockstroh S, Emre M, Tarral A and Pokorny R (1996) Effects of the novel NMDA-receptor antagonist SDZ EAA 494 on memory and attention in humans. *Psychopharmacology* **124:**261–266.
Rogawski MA (1993) Therapeutic potential of excitatory amino acid antagonists: Channel blockers and 2,3-benzodiazepines. *Trends Pharmacol Sci* **14:**325–331.
Schneggenburger R, Zhou Z, Konnerth A and Neher E (1993) Fractional contribution of calcium to the cation current through glutamate receptor channels. *Neuron* **11:**133–143.
Schubert H, Rack M and Mühlstädt M (1990) Eine vereinfachte synthese der 1-aminocyclopropan-1-carbonsäure. *J f Prakt Chemie* **332:**812–814.
Skolnick P, Marvizon J, Jackson B, Monn J, Rice K and Lewin A (1989) Blockade of N-methyl-D-aspartate induced convulsions by 1-aminocyclopropanecarboxylates. *Life Sci* **45:**1647–1655.
Sveinbjornsdottir S, Sander JWAS, Upton D, Thompson PJ, Patsalos PN, Hirt D, Emre M, Lowe D and Duncan JS (1993) The excitatory amino acid antagonist D-CPP-ene (SDZ EAA-494) in patients with epilepsy. *Epilepsy Res* **16:**165–174.
Szatkowski M and Attwell D (1994) Triggering and execution of neuronal death in brain ischaemia: Two phases of glutamate release by different mechanisms. *Trends Neurosci* **17:**359–365.
Vaidyanathan G and Wilson JW (1989) Decarboxylation of 1-aminocyclopropanecarboxylic acid and its derivatives. *J Org Chem* **54:**1810–1815.
Villarroel A, Regalado MP and Lerma J (1998) Glycine-independent NMDA receptor desensitization: Localization of structural determinants. *Neuron* **20:**329–339.
Watson GB and Lanthorn TH (1990) Pharmacological characteristics of cyclic homologues of glycine at the N-methyl-D-aspartate receptor-associated glycine site. *Neuropharmacology* **29:**727–730.

Send reprint requests to: Dr. Morris Benveniste, Department of Physiology and Pharmacology, Sackler School of Medicine, Tel Aviv University, Ramat Aviv 69978, Israel. E-mail: morrisb@post.tau.ac.il